scientific reports

Check for updates

OPEN

Ultrasound-based incidence of coarctation of the aorta in true and false positive fetuses

Guihong Chen[1]✉, Na Li[1], Zhenglun Alan Wei[2], Wei Zhao[1], Xijuan Guo[1], Yu Chen[1], Xuna Geng[1], Yuanyuan Peng[3], Bu-Lang Gao[4], Shuping Ge[5] & Jie Mi[4]✉

To investigate the incidence and significant ultrasound parameter changes of coarctation of the aorta (CoA) among fetuses with suspected CoA, pregnant women with suspected CoA fetuses on prenatal ultrasound examination were prospectively enrolled. The CoA presence was confirmed after birth by computed tomographic angiography, ultrasound, surgery or autopsies. The ultrasound parameters were analyzed. Among 133 fetuses with suspected CoA, 44 (33.1%) pregnant women with CoA fetuses were confirmed after delivery with an age range 20–41 (31.36 ± 4.73) years and a gestational age range 20.5–36.5 (27.35 ± 4.52) weeks, and 89 (66.9%) pregnant women were confirmed to have false-positive CoA fetuses with matched ($P > 0.05$) age (range 21–44 and mean 30.96 ± 4.59 years) and gestational age (range 19.6–34.1 and mean 28.22 ± 3.28 weeks). Ductus arteriosus (DA) tortuosity was present in significantly ($P < 0.05$) more false-positive CoA fetuses (15 or 16.85%) than in true CoA fetuses (1 or 2.27%), whereas significantly more intracardiac malformation [25 (56.82%) vs. 31 (34.83%)] and ventricular septal defect [10 (22.73%) vs. 6 (6.74%)] took place in true CoA fetuses than in the counterparts. Significant ($P < 0.05$) independent risk factors for CoA presence were sagittal view isthmic Z-score (odds ratio or OR 3.62 and 95% confidence interval or CI 2.06–7.15), coarctation shelf (OR 17.71 and 95% CI 5.52–56.78), ascending aortic diameter (OR 109.67 and 95% CI 3.03-21068.82), and DA velocity time integral (VTI) (OR 24.98 and 95% CI 1.26-759.94). The cutoff value and AUC were 0.40 and 0.912, respectively, for the fitted model, -4.24 and 0.779 for isthmus Z-score, 0.35 and 0.685 for the ascending aorta diameter, and 13.78 and 0.623 for DA VTI. In conclusion, many ultrasound parameters are significantly different in CoA fetuses, and sagittal view isthmus Z-score, coarctation shelf, ascending aortic diameter, DA VTI may independently affect CoA presence.

Keywords Coarctation of the aorta, Ultrasound parameter, False positive, Risk factors, Fetuses

Coarctation of the aorta (CoA) is featured by stenosis of the aortic isthmus, accounting for 6-8% of congenital cardiac diseases[1–7]. The CoA may cause cardiovascular collapse after birth and closure of the ductus arteriosus (DA), resulting in severe consequences. Antenatal confirmation of this condition may allow for immediate treatment and prevention of relevant complications, including prostaglandin therapy and early surgical correction. Nonetheless, the rate of antenatal diagnosis of CoA, especially the isolated ones, has been reported to be low, with a 38% false positive rate and a 60-80% false negative rate[6,8–11]. Miss-diagnosed CoA may lead to life-threatening consequences, and diagnosis with a high false positive rate may result in unnecessary admission to the intensive care unit and overuse of prostaglandin therapy. Some prenatal sonographic parameters have been suggested for prediction of CoA[3,6,11–14], including ventricular and arterial disproportion, aliasing or reversed blood flow across the aortic arch, caliber of the pulmonary artery (PA) or the aorta at the aortic valve, ascending aorta (AAO), aortic isthmus, ratio of the diameter between the PA and AAO or between the DA and aortic isthmus, presence of persistent left vena cava, coarctation shelf, and hypoplastic aortic arch. However, ultrasound parameters have not been investigated thoroughly for prenatal diagnosis of CoA (Fig. 1), and this study explored many ultrasound parameters in fetuses with different gestational ages for prenatal diagnosis of CoA.

[1]Medical Ultrasound Department, The Fourth Hospital of Shijiazhuang, No. 16 Tangu North Street, Shijiazhuang 050000, China. [2]Department of Biomedical Engineering, Worcester Polytechnic Institute, Worcester, USA. [3]Prenatal Diagnosis Center, Hebei Key Laboratory of Maternal and Fetal Medicine, The Fourth Hospital of Shijiazhuang, Shijiazhuang, China. [4]Cardiology Department, the people's Hospital of Shijiazhuang, No. 365, Jianhua South Street, Shijiazhuang 050026, Hebei, China. [5]Department of Pediatric, and Adult Congenital Cardiology, Geisinger Heart and Vascular Institute, Geisinger Medical Center, Danville, USA. ✉email: chenguihongn@sina.cn; mmmjjj2015@163.com

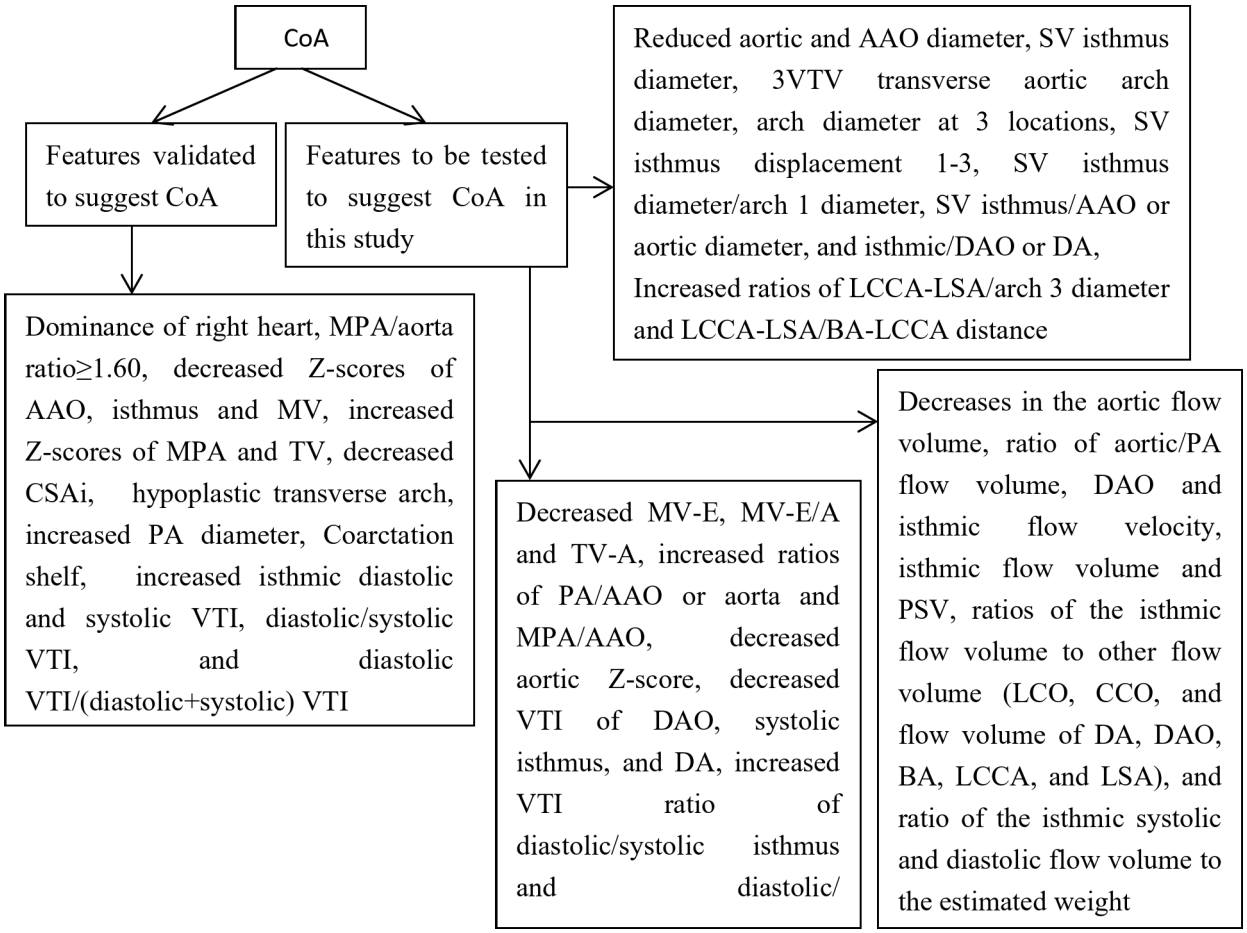

Fig. 1. Flow chart with the primary parameters validated in previous studies and new ones to be tested to suggest CoA in the current study. *CoA* coarctation of the aorta, *MPA* main pulmonary artery, *AAO* ascending aorta, *MV* mitral valve, *MV-E* mitral valve E peak; *TV* tricuspid valve; *TV-A* tricuspid valve A peak; *CSAi* carotid to subclavian artery index; *PA* pulmonary artery; *VTI* velocity time integral; *DAO* descending aorta; *DA* ductus arteriosus; *3VTV* Three vessel trachea view; *SV* sagittal view; *LCCA* left common carotid artery; *LSA* left subclavian artery; *BA* brachiocephalic artery; *PSV* peak systolic velocity; *LCO* left cardiac output; *CCO* combined cardiac output.

Materials and methods

Subjects

This prospective single-center study was conducted after approval by the ethics committee of the Fourth Hospital of Shijiazhuang, and all pregnant women had signed informed consent to participate. All methods were performed in accordance with the relevant guidelines and regulations. Pregnant women with 19–40 weeks of gestational age, regularity of menstrual cycles before gestation, prenatal ultrasound and physical examinations, and singleton pregnancy from June 2021 to June 2023 were enrolled. Inclusion criteria were pregnant women with singleton pregnancy, regularity of menstrual cycles before gestation, 19–40 weeks of gestational age, prenatal ultrasound examination, and follow-up for 6 months after delivery for confirmation of CoA in the fetuses by ultrasound, computed tomographic angiography (CTA), surgery, or autopsies on induced fetuses. The inclusion criteria for fetuses suspected of CoA were the ratio of DA inner diameter to aortic isthmic inner diameter > 1.3 and decreased isthmic diameter (Z-Score < -2) with or without aortic arch dysplasia (transverse arch diameter smaller than 1/2 of the abdominal aortic diameter) (Fig. 2). The exclusion criteria included pregnant women with twin pregnancies, hereditary diseases of the women, pregnancy complications, abnormal non-invasive prenatal test, unclear time of last menstrual cycle, irregularity of menstruation cycles before gestation, fetuses with concomitant severe cardiac abnormalities or presence of aortic arterial branch variations, or incomplete pre- and post-natal follow-up data.

Sonographic instruments

The GE Voluson E10 Color Doppler ultrasound diagnostic instrument (Austria) was used and equipped with 2D/3D transabdominal probes (frequency 2-5 MHz/4-8 MHz) of the model C1-6-D and RAB6-D and power < 100 mW/cm^2. The STIC software package was configured in the instrument, with 4D View 7.0 Offline analysis for fetal sonograhpic scan and measurement. Routine obstetric fetal ultrasound scan was conducted to

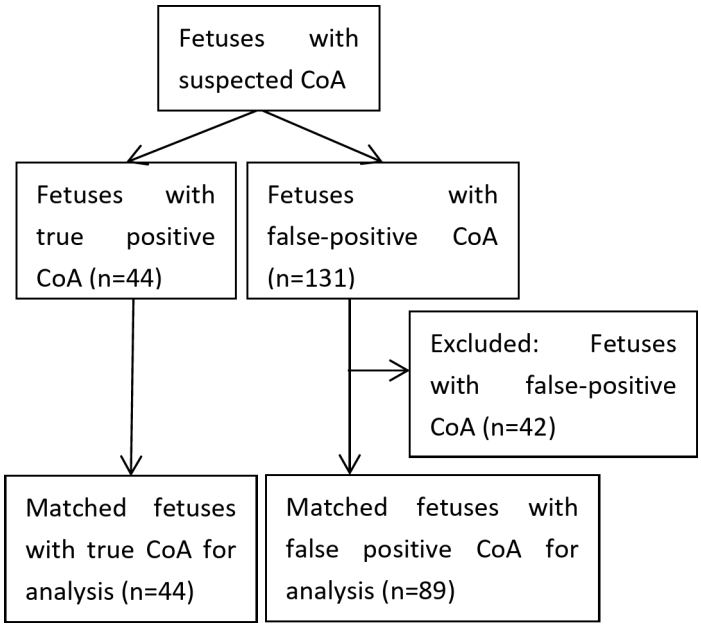

Fig. 2. Enrollment process of fetuses.

evaluate the fetal growth and development, condition, weight, and possible intra- and extracardiac abnormalities, and fetal echocardiography was performed according to the International Society of Ultrasound in Obstetrics and Gynecology (ISUOG) guidelines[15] and standards of fetal heart ultrasound screening (2023)[16]. Ultrasound images were collected, measured and calculated by two experienced ultrasound physicians with over 10 years of experience, and if in significant disagreement, a third senior author was involved to reach an agreement.

Ultrasound parameters

The fetal general biological data and blood flow parameters, including peak systolic velocity (PSV) and velocity time integral (VTI), were measured. Fetal systemic condition, placenta, amniotic fluid condition, fetal heart condition, and the accompanying abnormal conditions were checked up and recorded. The heart axis, cardio-thoracic ratio (Area/Circumference), right and left atrial end-systolic dimension, right and left ventricular end-diastolic dimension, mitral valve A-peak flow velocity (MV-A), mitral valve E-peak flow velocity (MV-E), tricuspid valve A peak (TV-A), and tricuspid valve E peak (TV-E) were measured in the four-chamber view. Systolic aortic valve annular diameter, AAO inner diameter, aortic flow velocity, PA diameter at the PA valve annulus, main pulmonary artery (MPA) inner diameter and PA flow velocity were measured at the left and right ventricular outflow tract sections. The spectrum automatic envelope was used to obtain the VTI, immediate heart rate, right cardiac output (RCO) or the PA flow volume, left cardiac output (LCO) or the aortic flow volume, and combined cardiac output (CCO = LCO + RCO) according to the formula Q/estimated fetal weight $=(D/2)^2 \times 3.14 \times VTI \times HR$ (immediate heart rate)/estimated fetal weight. The inner diameter of the aortic arch at locations of arch 1–3, aortic isthmus (sagittal view or SV) and descending aorta (DAO), and the distance between the left common carotid artery (LCCA) and the brachiocephalic artery (BA) or the left subclavian artery (LSA) at the origin were measured (Fig. 2). The flow rate of three arch branches, aortic isthmus and DAO was detected, and the frequency spectrum automatic envelope was applied to obtain each PSV, VTI, immediate heart rate and flow volume. The DA flow rate was measured in the DA arch, with the VTI and immediate heart rate automatically acquired.

When the long axis of the aortic arch blood flow was clearly demonstrated by the 2D-Doppler image, the 3D probe was selected in the real-time 3D STIC mode, with adjustment of the sampling box slightly greater than the lesion size, volume scanning angle of 30–45° and acquisition time 7–10 s. The breath was held before the STIC scanning with 3D volume data collected. In the Color Render mode, the HD live flow imaging mode was used to get the 3D image, and the CFM Sihou (transparency regulation) and Transp (vascular contour display clarity) keys were adjusted in line with the requirements to obtain the best image. The angle (from the bird's eye view and at the sagittal view), displacement 1 (the vertical distance between LSA and DAO), displacement 2 (the vertical distance between the aortic arch inlet and DAO), and displacement 3 (the vertical distance between the LSA and the aortic arch inlet) were measured (Fig. 3). All these measurements were conducted in the fetal quiet state without influencing by the fetal breathing movement.

Statistical analysis

The JMP software (10.01.2, SAS Institute, Cary, NC, USA) was used for the statistical analysis of this study. Continuous data were expressed as a mean and standard deviation and tested with the t test if in the normal distribution or a median and interquartile range if not in the normal distribution and tested with the Mann Whitney U test. Categorical variables were presented as frequency and percentage and tested with the Chi

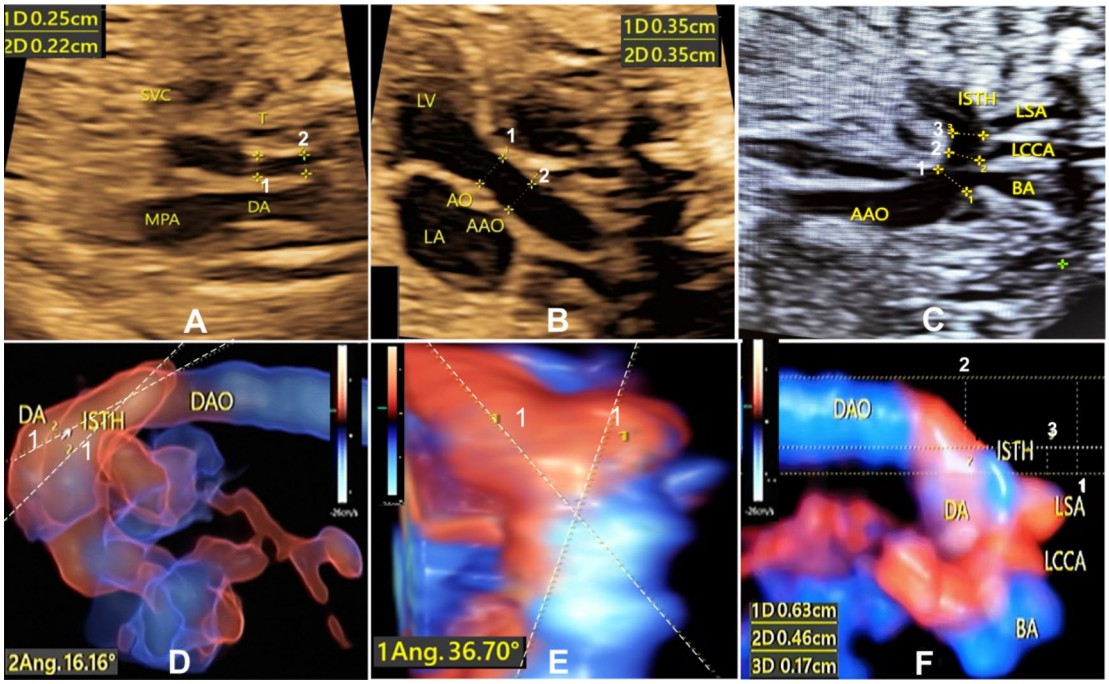

Fig. 3. Parameters measured on ultrasound images. (**A**) The transverse aorta (1) and the aortic isthmic (2) diameters were measured on the 3 vessel trachea view, with the transverse aorta diameter of 0.25 cm and the isthmic diameter of 0.22 cm. (**B**) The aorta (AO) diameter at the aortic valve annulus and the ascending aorta (AAO) diameter were measured at the left ventricular outflow tract section, with the AO diameter (1) of 0.35 cm and the AAO diameter of 0.35 cm. (**C**) The aortic arch diameter was measured at arch 1 before the brachiocephalic artery (BA), arch 2 before the left common carotid artery (LCCA) and arch 3 before the left subclavian artery (LSA). (**D**) The DA-isthmus angle was measured on the HD Live Flow image on the sagittal view, with the DA-Isthmus angle of 16.16°. (**E**) The DA-isthmus angle was measured on the 3D STIC HD Live Flow image viewed from the superior aspect, with the DA -Isthmus angle of 36.70°. (**F**) Displacements 1–3 were measured on the 3D STICK-HD Live Flow image. Displacement 1: the vertical distance between the LSA origin and the outer edge of the descending aorta (DAO), displacement 2: the vertical distance between the aortic arch import point on the aorta (or isthmus-DA junction) and the DAO outer edge, and displacement 3: the vertical distance between the LSA origin and the Isthmus-DA junction. *DA* ductus arteriosus; *MPA* main pulmonary artery; *SVC* superior vena cava; *ISTH* aortic isthmus.

square test. Risk factors of CoA presence were analyzed using the univariate logistic regression analysis, and the multivariate regression analysis was conducted for independent risk factors of CoA using the significant ($P<0.05$) factors in the univariate analysis after elimination of confounding factors. The receiver operating characteristics (ROC) curve analysis was performed for continuous independent risk factors for CoA, with calculation of the cutoff value, area under the ROC curve (AUC), specificity, sensitivity, positive (PPV) and negative predictive value (NPV), and Youden index. $P<0.05$ was used as the statistical significant value.

Results

Totally, 44 pregnant women with CoA fetuses were confirmed after delivery with an age range 20–41 (31.36 ± 4.73) years and a gestational age range 20.5–36.5 (27.35 ± 4.52) weeks, and 89 pregnant women with false-positive CoA fetuses were enrolled as the false positive group with matched ($P>0.05$) age (range 21–44 and mean 30.96 ± 4.59 years) and gestational age (range 19.6–34.1 and mean 28.22 ± 3.28 weeks) (Table 1). The fetal general biological measurement data were matched ($P>0.05$) between the CoA positive and false-positive groups. Follow-up medical images (including CTA and ultrasound), surgery or autopsies after birth confirmed the presence of CoA in all 44 CoA positive fetuses but no CoA in the false-positive CoA fetuses (Figs. 4 and 5). In the CoA positive fetuses compared with the false-positive ones (Figs. 4 and 5), a significant ($P<0.05$) decrease was detected in MV-E, MV-A, MV-E/A, TV-E, TV-A, isthmus diameter and Z-score (SV), isthmus (SV)/DA diameter, transverse aortic arch diameter, arch diameters at arch locations 1–3, SV isthmic diameter/arch 1 diameter, SV isthmic diameter/AAD or AD, LSA-DAO isthmic displacement between LSA and DAO on HD live flow, and isthmic displacement 3 between the LSA and the aortic arch inlet (Table 2).

In the true CoA fetuses (Table 3), a significant ($P<0.05$) increase was found in the ratio between the LCCA-LSA distance and arch 3 diameter or between the LCCA-LSA distance and BA-LCCA distance, PA/AAO, PA/AO, and MPA/AAO, whereas a significant ($P<0.05$) decrease was detected in the aortic and AAO diameter and Z scores, aortic flow volume, aortic flow/PA flow volume, DAO flow velocity and VTI.

Groups		Positive	False-positive	*P*
Pregnant women	Age (y)	20–41 (31.36 ± 4.73)	21–44 (30.96 ± 4.59)	0.79
	Gestational age (w)	20.5–36.5 (27.35 ± 4.52)	19.6–34.1 (28.22 ± 3.28)	0.13
Fetuses	BPD (cm)	4.72–9.36 (7.0 ± 1.24)	4.74–9.63 (7.28 ± 0.96)	0.10
	HC (cm)	1793 – 33.57 (25.42 ± 4.26)	17.16–31.44 (25.45 ± 4.40)	0.12
	AC(cm)	15.16–34.65 (22.86 ± 4.84)	14.82–31.1 (23.74 ± 3.49)	0.15
	FL (cm)	3.27–7.16 (4.95 ± 1.10)	3.03–6.6 (5.23 ± 0.76)	0.06
	HL (cm)	3.11–6.05 (4.47 ± 0.86)	3.03–5.78 (4.67 ± 0.61)	0.08
	Estimated weight (g)	359–3286 (1191.48 ± 731.50)	347.1–2476 (1237.79 ± 506.31)	0.54

Table 1. General data of the patients. Normal control, without vascular abnormality; Positive, CoA (coartaction of the aorta) positive; false-positive (no CoA) groups; suspected group: suspected of CoA including patients in the positive and false-positive group. *BPD* biparietal diameter, *HC* head circumference, *AC* abdomen circumference, *FL* femur length, *HL* humerus length.

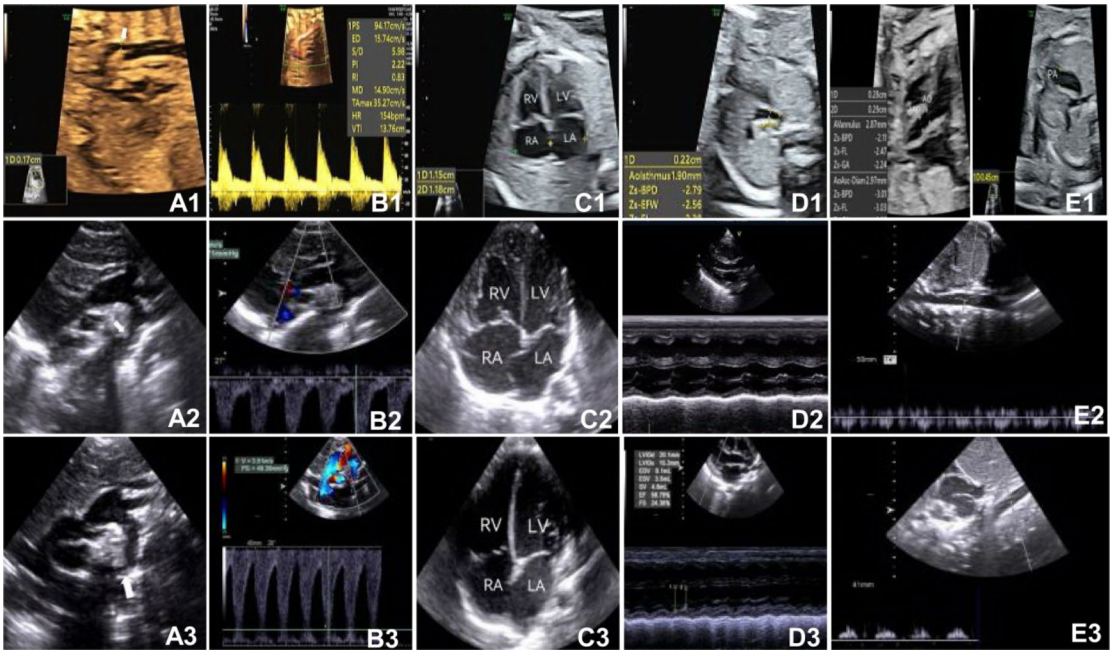

Fig. 4. A baby with true coarctation of the aorta (CoA) before and after birth. (**A1**-**E1**) Fetal ultrasound image at the gestational age 24 weeks and 6 days after birth. (**A1**) In the aortic arch long axis section, a "stent sign" was shown in the aortic isthmus whose inner diameter was 0.17 cm (Z-Score: -3.65). (**B1**) The isthmic blood flow spectrum was normal with no obvious reflux. (**C1**) The left and right heart ratio was normal with the left atrial transverse diameter of 1.15 cm and right atrial transverse diameter of 1.18 cm. (**D1**) In the three vessel tracheal section, the isthmic inner diameter was 0.19 cm, and the aortic transverse arch inner diameter was 0.22 cm. (**E1**) The ratio of the pulmonary valve annulus diameter to the aortic valve annulus diameter was increased, and the aortic valve diameter was 0.28 cm (left) and the pulmonary artery was 0.45 cm (right). (**A2**-**E2**) Ultrasound images 35 h after birth before the closure of the ductus arteriosus (DA). (**A2**) The shape of the aortic arch is irregular, with a tortuous and thin inner diameter of 0.22 cm near the descending aorta at the distal end of the arch (→: thinner isthmus). (**B2**) The diastolic blood flow spectrum at this location increased with a peak systolic velocity (PSV) of 1.56 m/s at the isthmus and a pressure difference of 9.71 mmHg. (**C2**) The right heart is slightly larger. (**D2**) The left ventricular systolic function is normal with an ejection fraction (EF) of 63.02% and fraction of shortening (FS) 31.15%. (**E2**) The abdominal aortic spectrum showed a "small slow wave". (**A3**-**E3**) Ultrasound images forty-two days after birth with closure of the DA. (**A3**) The distal end of the descending part of the aortic arch was thin, with an inner diameter of 0.23 cm (→: thinner isthmus). (**B3**) The flow velocity was significantly increased with a PSV 3.51 m/s and a pressure difference of 49.36mmHg. (**C3**) The left ventricle was slightly larger in the four chamber view. (**D3**) The left ventricular systolic function was reduced with an EF 56.79% and FS 24.38%. (**E3**) The abdominal aortic spectrum was a "small slow wave". *LA* left atrium, *LV* left ventricle, *RA* right atrium, *RV* right ventricle, *AO* aorta, *AA0* ascending aorta, and *PA* pulmonary artery.

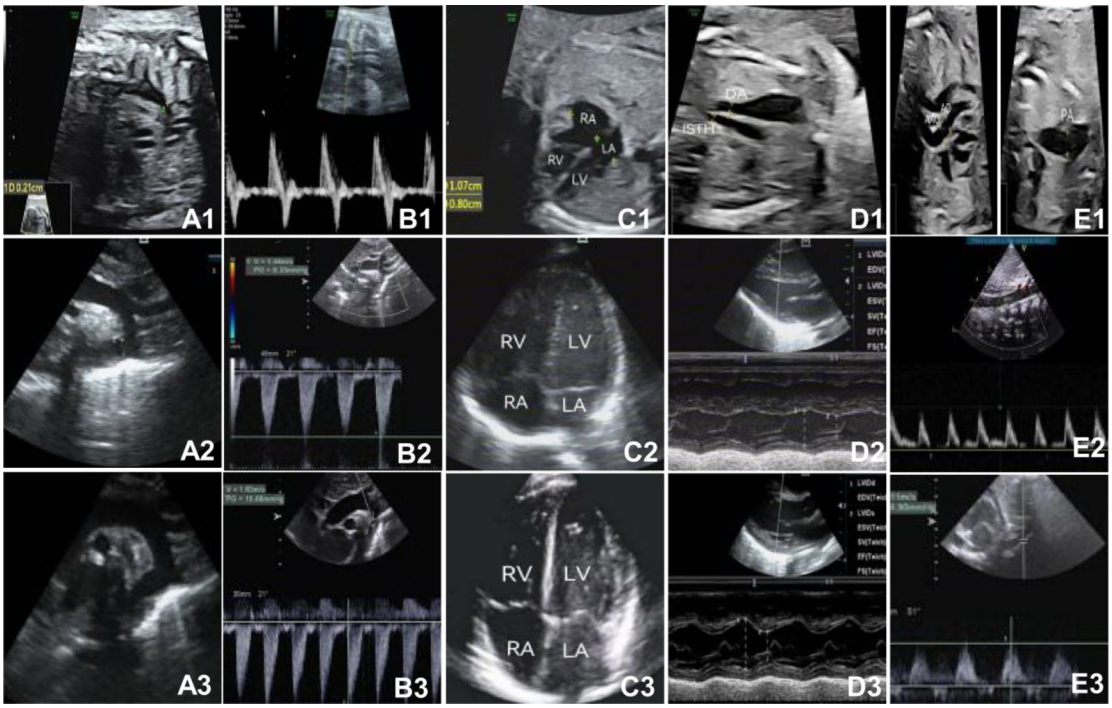

Fig. 5. A baby with false-positive coarctation of the aorta (CoA) before and after birth. (**A1**-**E1**) Ultrasound images of a fetus at the gestational age 25 weeks and 6 days after birth. (**A1**) In the aortic arch long axis section, a slightly thinner aortic isthmus was shown with an inner diameter of 0.21 cm (Z-Score: -2.92). (**B1**) The isthmic blood flow spectrum showed a retrograde flow in the late systole and early diastole. (**C1**) The right heart ratio was slightly larger, with the left atrial transverse diameter of 0.80 cm and right atrial transverse diameter of 1.07 cm. (**D1**) In the three vessel tracheal section, the isthmic inner diameter was 0.20 cm, and the inner diameter of the ductus arteriosus (DA) was 0.26 cm. (**E1**) The ratio of the pulmonary valve annulus diameter to the aortic valve annulus diameter was increased, with the aortic diameter of 0.34 cm (left) and pulmonary artery 0.53 cm (right). (**A2**-**E2**) Ultrasound images 31 h after birth without closure of the DA were shown. (**A2**) The shape of the aortic arch was normal, with an aortic isthmus inner diameter of 0.33 cm. (**B2**) The isthmic blood flow spectrum and velocity were normal with the peak systolic velocity (PSV) 1.44 m/s and a pressure difference 8.33 mmHg. (**C2**) The right heart was slightly larger. (**D2**) The left ventricular systolic function was normal with an ejection fraction (EF) 77.0% and fraction of shortening (FS) 42.2%. (**E2**) The abdominal aortic spectrum and velocity were normal with a PSV 0.65 m/s. (**A3**-**E3**) Ultrasound images 19 days and 8 h after birth with closure of the DA were demonstrated. (**A3**) The morphology of the aortic arch was regular, with an increase in the inner diameter of the aortic isthmus. (**B3**) The blood flow spectrum and velocity in the aortic isthmus were normal with a PSV of 1.63 m/s and a pressure difference of 10.68 mmHg. (**C3**) The size and ratio of the atria and ventricles in the four chamber view were normal. (**D3**) The left ventricular systolic function was normal with an EF 77.9% and FS 43.6%. (**E3**) The abdominal aortic spectrum and velocity were normal with a PSV of 1.11 m/s. *LA* left atrium, *LV* left ventricle, *RA* right atrium, *RV* right ventricle, *DA* ductus arteriosus, *ISTH* isthmus, *AO* aorta, *AAO* ascending aorta, *PA* pulmonary artery.

In the CoA fetuses (Table 4), significant ($P<0.05$) decreases were detected in the isthmic diameter/DAO diameter, isthmic PSV (total), isthmic flow volume, isthmic systolic velocity and VTI, isthmic systolic flow volume, isthmic diastolic flow/weight, and ratios of the isthmic flow volume to the left cardiac output, CCO, and flow volume of aorta, DA, DAO, BA, LCCA, and LSA. The DA VTI and LSA PSV were also significantly ($P<0.05$) decreased in the CoA positive fetuses than in the false-positive ones (Table 5).

The DA tortuosity was present in significantly ($P<0.05$) more false-positive fetuses (15 or 16.85%) than in true CoA fetuses (1 or 2.27%), whereas significantly ($P<0.05$) more intracardiac malformation [25 (56.82%) vs. 31 (34.83%)], ventricular septal defect [10 (22.73%) vs. 6 (6.74%)], extracardiac malformation [28 (63.6%) vs. 26 (29.2%)], and short limbs [13 (29.5%) vs. 11 (12.4%)] took place in the true CoA fetuses than in the counterparts. No significant ($P>0.05$) difference was detected in the rate of arch branch variations (5.62% vs. 6.82%) and permanent superior vena cava (1.12% vs. 2.3%) in the false-positive fetuses compared with those in the CoA fetuses.

The umbilical cord around the fetal neck (CAFN) was present in 8 (18.2%) of 44 CoA positive fetuses and in 31 (34.8%) of 89 CoA false-positive fetuses, with a significantly ($P=0.04$) increased rate in the CoA false-positive fetuses (Fig. 6). However, CAFN did not result in significant ($P>0.05$) differences in any parameters in the false-positive CoA fetuses, whereas in the true CoA fetuses, CAFN coexisted with significant ($P<0.05$) decreases in the isthmic flow velocity and PSV only. The univariate analysis (Table S1) revealed that significant ($P<0.05$) positive risk factors for CoA were weight%, MV-E, MV-E/A, TV-E, TV-A, isthmic diameter and

Variables	Positive	False-positive	*P*
Cardiac axis (°)	9.78–68.95 (42.75 ± 10.44)	24.16–60.98 (43.45 ± 8.09)	0.80
CTR	0.19–0.33 (0.27 ± 0.03)	0.21–0.41 (0.28 ± 0.04)	0.83
CTCR	0.45–0.58 (0.53 ± 0.04)	0.46–0.63 (0.53 ± 0.03)	0.96
Left atrium (cm)	0.55–1.43 (0.94 ± 0.21)	0.58–11.7 (0.96, 0.23)	0.39
Right atrium (cm)	0.7–1.8 (1.24 ± 0.27)	0.75–12.1 (1.23, 0.4)	0.40
Right atrium/left atrium	1-1.77 (1.36 ± 0.22)	0.95–2.20 (1.32 ± 0.25)	0.63
Left ventricle (cm)	0.5–1.49 (0.91 ± 0.28)	0.55–1.45 (0.96 ± 0.16)	0.11
Right ventricle (cm)	0.73–1.83 (1.15 ± 0.28)	0.62–1.81 (1.21 ± 0.26)	0.16
Right ventricle/left ventricle	0.90–2.14 (1.32 ± 0.26)	0.90–2.31 (1.26 ± 0.24)	0.32
MV-E (cm/s)	22.23–55.74 (36.23 ± 6.96)	24.14–67.68 (39.426 ± 7.58)	0.01
MV-A (cm/s)	35.96–80.69 (55.38 ± 10.05)	39.62-103.81 (56.25 ± 9.55)	0.48
MV-E/A	0.52–0.86 (0.67 ± 0.07)	0.48–0.90 (0.70 ± 0.08)	0.004
TV-E (cm/s)	23.39–52.62 (39.24 ± 6.90)	23.51–62.98 (43.13 ± 7.53)	0.003
TV-A (cm/s)	33.52–76.58 (56.90 ± 10.13)	41.16–88.42 (62.52 ± 9.10)	< 0.001
TV-E/A	0.52–0.84 (0.71 ± 0.07)	0.38–0.88 (0.70 ± 0.08)	0.74
DA diameter (cm)	0.21–0.7 (0.41 ± 0.11)	0.25–0.56 (0.39 ± 0.08)	0.45
Isthmus diameter (3VTV) (cm)	0.09–0.96 (0.22 ± 0.12)	0.16–0.32 (0.22 ± 0.04)	0.06
Isthmus diameter (SV) (cm)	0.08–0.31 (0.18 ± 0.04)	0.14–0.38 (0.24 ± 0.05)	< 0.001
Isthmus Z-score (SV)	-7.53- -2.14 (-5.05 ± 1.22)	-6.14- -1.22 (-3.80 ± 1.10)	< 0.001
Isthmus (3VTV)/DA	0.3–3.84 (0.43, 0.13)	0.38–0.82 (0.63 ± 0.10)	0.26
Isthmus (SV)/DA	0.26–0.83 (0.44 ± 0.11)	0.36–0.79 (0.58 ± 0.10)	< 0.001
Transverse aortic arch (3VTV) (cm)	0.11–0.44 (0.23 ± 0.08)	0.2–0.45 (0.29 ± 0.05)	< 0.001
Arch diameter 1 (cm)	0.18–0.56 (0.36 ± 0.11)	0.23–0.58 (0.40 ± 0.08)	0.006
Arch diameter 2 (cm)	0.11–0.44 (0.24 ± 0.08)	0.15–0.46 (0.28 ± 0.06)	< 0.001
Arch diameter 3 (cm)	0.08–0.39 (0.22 ± 0.06)	0.16–0.41 (0.26 ± 0.05)	< 0.001
Arch diameter 3/2	0.58–1.14 (0.92 ± 0.11)	0.7–1.16 (0.93 ± 0.10)	0.33
SV isthmus diameter/arch 1 diameter	0.32–0.71 (0.49 ± 0.11)	0.39–0.84 (0.56 ± 0.10)	< 0.001
SV isthmus diameter/arch 2 diameter	0.43–1.2 (0.76 ± 0.17)	0.52–1.08 (0.80 ± 0.13)	0.10
SV isthmus diameter/arch diameter 3	0.45–1.41 (0.82 ± 0.18)	0.59–1.24 (0.86 ± 0.13)	0.22
SV isthmus diameter/AAD	0.30–0.68 (0.48 ± 0.08)	0.4–0.70 (0.55 ± 0.07)	< 0.001
SV isthmus diameter/AD	0.30–0.68 (0.52 ± 0.09)	0.42–0.78 (0.58 ± 0.08)	< 0.001
3D isthmus displacement 1-LSA-DAO (cm)	0.03–0.8 (0.35 ± 0.16)	0.11–0.66 (0.27 ± 0.11)	0.006
3D DA-isthmus (above view) (°)	18.54–71.27 (32.26 ± 11.14)	10.22-120.38 (28.80 ± 13.11)	0.15
3D DA-Isthmus (SV) (°)	11.68–50.32 (27.67 ± 10.11)	4.76–68.2 (25.91 ± 13.38)	0.49
3D isthmus displacement 3- LSA-AORTIC ARCH INLET (cm)	0-0.67 (0.17,0.26)	0.07–0.67 (0.28 ± 0.13)	0.01

Table 2. Data of fetus heart, DA, and aortic isthmus in different groups. *CTR* cardiothoracic area ratio, *CTCR* cardiothoracic circumference ratio, *DA* ductus arteriosus, *MV-E* mitral valve E-peak flow velocity, *MV-A* mitral valve A-peak flow velocity, *TV-E* tricuspid valve E peak, *TV-A* tricuspid valve A peak, *DA* ductus arteriosus, *isthmus* aortic isthmus, *3VTV* three vessel trachea view, *SV* sagittal view, *AAD* ascending aortic inner diameter, *AD* aortic inner diameter, *LSA-DAO* left subclavian artery-descending aorta, *3D* HD live flow image.

Z-score, isthmic diameter/DA diameter, transverse arch diameter, arch 1–3 diameter, ratios of isthmic diameter to that of arch 1, AAO or AO, 3D isthmic displacement of LSA to DAO, 3D isthmic displacement to LSA-arch junction, Coarctation shelf, aortic Z-score, AAO diameter and Z-score, ratio of AO flow volume to weight or PA flow volume, SV isthmic diameter/DAO diameter, DAO flow velocity and VTI, DAO flow volume/weight, isthmic flow PSV (of the entire cardiac cycle), isthmic flow volume, isthmic flow volume to other parameters (weight, LCO, CCO, and flow volume of DA, AO, DAO, BA, LCCA and LSA), isthmic systolic flow velocity and VTI, isthmic systolic flow volume, isthmic systolic flow volume/weight, isthmic diastolic flow volume, isthmic diastolic flow volume/weight, ratio of isthmic diastolic VTI to isthmic systolic or isthmic total VTI, DA VTI, and LSA PSV. Significant ($P < 0.05$) negative risk factors for CoA were 3D isthmic displacement LSA-DAO, 3D isthmus-DAO displacement, ratio of LCCA-LSA distance to arch 3 diameter or BA-LCCA distance, ratio of PA diameter to AAO or aortic diameter, MPA/AAO diameter, and ratio of isthmic diastolic VTI to isthmic systolic VTI or total VTI.

The multivariate logistic regression analysis showed that significant ($P < 0.05$) independent risk factors for CoA presence were SV isthmic Z-score (OR 3.62 and 95% CI 2.06–7.15), coarctation shelf (OR 17.71 and 95% CI 5.52–56.78), AAO diameter (OR 109.67 and 95% CI 3.03-21068.82), and DA VTI (OR 24.98 and 95% CI 1.26-759.94). The ROC curve analysis of the whole fitted model for the multivariate analysis revealed that the cutoff

Variables	Positive	False-positive	*P*
BA (cm)	0.09–0.42 (0.22 ± 0.07)	0.1–0.35 (0.22 ± 0.06)	0.38
LCCA (cm)	0.11–0.35 (0.18 ± 0.07)	0.09–0.29 (0.20 ± 0.05)	0.65
LSA (cm)	0.07–0.27 (0.17 ± 0.04)	0.08–0.35 (0.18 ± 0.04)	0.17
BA-LCCA distance	0-0.03 (0.12 ± 0.04)	0.04–0.25 (0.12 ± 0.05)	0.18
LCCA-LSA distance (cm)	0.06–0.63 (0.28 ± 0.16)	0.07–0.56 (0.23 ± 0.10)	0.07
LCCA-LSA/AO diameter at arch 3	0.29–3.71 (1.09, 1,14)	0.24–2.67 (0.92 ± 0.44)	< 0.001
LCCA-LSA/BA-LCCA	0.42–12.6 (2.44, 301)	0.4-8 (2.07,1.50)	0.03
AO diameter (cm)	0.15–0.56 (0.34 ± 0.11)	0.23–0.52 (0.39 ± 0.06)	< 0.001
AO Z-score	-5.76-0.52 (-2.58, 2.12)	-4.29-0.35 (-1.51,0.82)	< 0.001
AAO diameter (cm)	0.16–0.61 (0.36 ± 0.11)	0.24–0.55 (0.40 ± 0.06)	0.002
AAO Z-score	-5.93- − 0.45 (-2.92 ± 1.21)	-4.2-1.77 (-1.97 ± 0.81)	< 0.001
Aortic flow velocity (cm/s)	60.26-126.02 (87.60 ± 14.74)	59.73-125.22 (88.23 ± 12.80)	0.65
Aortic VTI (cm)	8.67–20.26 (12.59 ± 2.24)	7.86–18.48 (12.73 ± 2.08)	0.59
AO flow volume (ml/min)	31.11-556.52 (137.36, 130.11)	70.29-430.08 (216.70 ± 84.64)	0.04
AO flow volume/weight (ml/min/g)	0.08–0.31 (0.16 ± 0.04)	0.09–4.53 (0.17, 0.07)	0.28
PA diameter (cm)	0.28–0.89 (0.55 ± 0.17)	0.35–0.82 (0.54 ± 0.10)	0.83
PA Z-score	-2.6-1.75 (-0.01, 1.21)	-2.64-1.6 (-0.37, 1.35)	0.49
MPA diameter (cm)	0.38–1.37 (0.73 ± 0.22)	0.42–1.02 (0.73 ± 0.13)	0.80
MPA Z-score	-1-2.9 (1.13, 0.65)	-1.14-2.54 (1.12, 0.85)	0.67
MPA PSV (cm/s)	54.63-106.44 (71.37 ± 11.26)	47.93–95.8 (70.07 ± 10.93)	0.69
PA VTI (cm)	7.29–17.45 (11.49 ± 2.23)	7.62–16.73 (11.68 ± 1.81)	0.47
PA flow volume (ml/min)	92.46-1269.49 (325.01, 423.13)	115.65-1036.03 (407.73 ± 181.46)	0.47
PA flow volume/weight (ml/min/g)	0.22–0.60 (0.38 ± 0.07)	0.17–8.16 (0.32, 0.1)	0.17
Flow volume of AO /PA	0.18–0.88 (0.44 ± 0.14)	0.25–1.05 (0.57 ± 0.17)	< 0.001
CCO (ml/min)	123.57-1826.01 (463.63,567.24)	187.27-1329.13 (624.43 ± 247.82)	0.92
CCO/weight (ml/min/g)	0.32–0.72 (0.51 ± 0.11)	0.32–12.69 (0.51, 0.15)	0.52
PA/AAO	1.10–2.09 (1.56 ± 0.25)	1.04–1.82 (1.35 ± 0.18)	< 0.001
PA/AO	1.13–2.23 (1.66 ± 0.25)	1.12–2.11 (1.43 ± 0.20)	< 0.001
MPA/AAO	1.42–2.92 (2.06 ± 0.35)	1.33–2.59 (1.88 ± 0.26)	< 0.001
DAO-Z-score	-3.22-0.59 (-0.88, 1.24)	-2.99-1.03 (-0.72, 1.11)	0.15
DAO diameter (cm)	0.21–0.65 (0.41 ± 0.11)	0.24–0.58 (0.41 ± 0.07)	0.33
DAO velocity (cm/s)	64.78-135.26 (90.86 ± 16.76)	47.63-197.44 (100.62 ± 24.35)	0.01
DAO VTI (cm)	9.96–19.63 (14.23 ± 2.74)	7.5-32.98 (16.33 ± 4.21)	0.004
DAO flow volume (ml/min)	62.35-834.68 (237.60, 274.21)	85.02–851.60 (336.71 ± 161.55)	0.15
DAO flow volume/ weight (ml/min/g)	0.16–0.35 (0.25 ± 0.06)	0.15–6.96 (0.26, 0.1)	0.35

Table 3. Data of fetal three arteries on the aortic arch, aorta, and pulmonary artery. *BA* brachiocephalic artery trunk, *LCCA* left common carotid artery, *LSA* left subclavian artery, *AO* aorta, *AAO* ascending aorta, *VTI* velocity time integral, *PA* pulmonary artery, *MPA* main pulmonary artery, *3VTV* Three vessel trachea view, *SV* sagittal view, *LCO* left cardiac output, *CCO* combined cardiac output, *DAO* descending aorta, *PSV* peak systolic velocity.

value and AUC were 0.40 and 0.912, respectively, with a sensitivity 0.864, specificity 0.909, positive predictive value (PPV) 0.826, negative predictive value (NPV) 0.930, and Youden index 0.773 (Fig. 7A).

The ROC curve analysis of continuous independent risk factors for CoA presence (Fig. 7) revealed that the cutoff value, AUC, sensitivity, specificity, PPV, NPV, and Youden index were − 4.24, 0.779, 0.796, 0.697, 0.565, 0.873, and 0.493, respectively, for SV isthmic Z-score, 0.35, 0.685, 0.591, 0.775, 0.565, 0.793, and 0.276 for AAO diameter, and 13.78, 0.623, 0.727, 0.551, 0.444, 0.803, and 0.278 for DA VTI.

Discussion

In this study exploring the incidence and significant ultrasound parameter changes of CoA among fetuses with suspected CoA, it was found that many ultrasound parameters were significantly different in CoA fetuses and that sagittal view isthmus Z-score, coarctation shelf, ascending aortic diameter, and DA VTI independently affected CoA presence.

The CoA in fetuses is linked to subtle and inconsistent characteristics in the mid-trimester and is also the commonest ductal-dependent disease missed on neonatal examination screening[7,17]. Because CoA is frequently a progressive disease and may resemble normal physiological alterations in the fetal hemodynamics at the late gestation, false-positive and false-negative diagnoses may occur, leading to a disadvantageous impact on the postnatal management. False-negative diagnosis of CoA may result in neonatal cardiovascular deterioration,

Variables	Positive	False-positive	*P*
Isthmus (3VTV)/DAO diameter	0.37–3.57 (0.56 ± 0.47)	0.38–0.84 (0.59 ± 0.09)	0.63
Isthmus (SV)/DAO diameter	0.31–0.63 (0.44 ± 0.08)	0.36–0.81 (0.54 ± 0.09)	< 0.001
Isthmus velocity PSV (Total) (cm/s)	37.82-110.51 (71.42 ± 20.28)	29.38-108.31 (78.29 ± 15.53	0.03
Isthmus VTI (cm)	5.11–22.3 (11.29 ± 3.85)	5.61-18 (11.88 ± 2.72)	0.24
Isthmus flow volume (ml/min)	5.21-132.97 (41.98 ± 28.99)	19.97–165.90 (68.65 ± 32.48)	< 0.001
Isthmus flow volume/weight (ml/min/g)	0.01–0.09 (0.04 ± 0.02)	0.01–2.08 (0.06, 0.03)	0.18
Isthmus flow volume/LCO	0.07–0.49 (0.25 ± 0.11)	0.09–0.69 (0.33 ± 0.12)	< 0.001
Isthmus flow volume/CCO	0.02–0.19 (0.08 ± 0.03)	0.02–0.32 (0.12 ± 0.05)	< 0.001
Isthmus flow/DA flow volume	0.05–0.58 (0.18 ± 0.11)	0.08–0.87 (0.31 ± 0.15)	< 0.001
Isthmus flow/AO flow	0.07–0.49 (0.25 ± 0.11)	0.09–0.69 (0.33 ± 0.12)	< 0.001
Isthmus flow volume/DAO flow volume	0.04–0.38 (0.15 ± 0.07)	0.06–0.78 (0.23 ± 0.10)	< 0.001
Isthmus flow volume/BA flow volume	0.10–4.69 (0.98 ± 0.81)	0.16–6.97 (1.17, 0.91)	0.02
Isthmus flow volume/LCCA flow volume	0.26–3.53 (1.21 ± 0.84)	0.25–7.95 (1.74, 1.25)	< 0.001
Isthmus flow volume/LSA flow volume	0.28–5.88 (1.12, 1.31)	0.37–12.83 (1.84, 1.0)	0.03
Isthmus systolic velocity (cm/s)	24.64-109.55 (72.46 ± 20.89)	29.42-110.45 (80.62 ± 15.92)	0.01
Isthmus systolic VTI (cm)	1.78–16.56 (7.17 ± 2.89)	1.47–17.63 (8.24 ± 2.27)	0.02
Isthmus systolic flow volume (ml/min)	3.13–91.14 (23.19,24.47)	8.65-109.21 (47.53 ± 22.87)	< 0.001
Isthmus systolic flow volume/weight (ml/min/g)	0.004-006 (0.02 ± 0.01)	0.004–1.39 (0.04, 0.02)	0.15
Isthmus diastolic velocity (cm/s)	17.21–66.12 (29.69 ± 9.61)	8.9-48.93 (25.94 ± 7.28)	0.01
Isthmus diastolic VTI (cm)	2.38–10.17 (4.40 ± 1.89)	1.2–8.37 (4.03 ± 1.24)	0.21
Isthmus diastolic flow volume (ml/min)	2.14–39.53 (8.26, 8.03)	4.92–64.85 (23.31 ± 12.48)	0.29
Isthmus diastolic flow/weight (ml/min/g)	0.01–0.03 (0.01 ± 0.004)	0.004–0.78 (0.02, 0.01)	< 0.001
Isthmus diastolic VTI/systolic VTI	0.31–5.03 (0.61, 0.40)	0.17–3.13 (0.49, 0.20)	0.01
Isthmus diastolic VTI/isthmus total VTI	0.24–1.04 (0.42 ± 0.15)	0.15–1.14 (0.34 ± 0.11)	0.01

Table 4. Isthmus data. *3VTV* Three vessel trachea view; *SV* sagittal view; *DAO* descending aorta; *DA* ductus arteriosus; *PSV* peak systolic velocity; *VTI* velocity time integral; *LCO* left cardiac output; *CCO* combined cardiac output; *AO* aorta; *DAO* descending aorta; *BA* brachiocephalic artery trunk; *LCCA* left common carotid artery; *LSA* left subclavian artery.

Variables	Positive	False-positive	*P*
DA PSV (cm/s)	51.37-131.46 (87.82 ± 18.60)	55.74-146.17 (94.08 ± 19.98)	0.06
DA VTI (cm)	8.29–17.35 (12.76 ± 2.35)	8.26–22.01 (14.19 ± 3.3)	0.01
DA flow (ml/min)	62.83-659.33 (208.23, 221.31)	74.92-693.56 (258.88 ± 120.52)	0.95
DA flow/weight (ml/min/g)	0.15–0.44 (0.24 ± 0.06)	0.11–0.52 (0.20 ± 0.08)	0.07
BA-PSV (cm/s)	48.14-370.27 (89.52 ± 44.09)	49.93-235.39 (95.14 ± 31.07)	0.42
BA VTI (cm)	5.27–46.05 (9.58, 6.31)	5.17–29.14 (10.76 ± 3.89)	0.77
BA flow (ml/min)	7.88-361.03 (41.24, 63.15)	7.02-283.95 (59.15,45.3)	0.88
BA flow/weight (ml/min/g)	0-0.23 (0.04, 0.02)	0.01–1.96 (0.05, 0.03)	0.45
LCCA-PSV (cm/s)	42.19-195.53 (80.56 ± 26.02)	38.22-325.57 (91.32 ± 36.35)	0.09
LCCA VTI (cm)	5.58–20.74 (9.95 ± 3.02)	4.2-37.93 (10.81 ± 4.47)	0.25
LCCA flow (ml/min)	8.27-159.18 (32.97, 62.32)	6.16-222.96 (35.68, 35.21)	0.77
LCCA flow/weight (ml/min/g)	0-0.08 (0.04 ± 0.01)	0.01–1.05 (0.03, 0.02)	0.56
LSA PSV (cm/s)	46.32-155.59 (80.88 ± 22.22)	44.92–189.8 (92.85 ± 23.82)	0.01
LSA VTI (cm)	4.95–16.36 (9.37 ± 2.58)	3.8-20.57 (10.31 ± 2.76)	0.06
LSA flow (ml/min)	4.69-132.18 (23.57, 29.88)	5.28-165.34 (34.08,24.1)	0.20
LSA flow/weight (ml/min/g)	0-0.05 (0.03 ± 0.01)	0.01–0.83 (0.03, 0.02)	0.31

Table 5. PSV, VTI, and flow data. *PSV* peak systolic velocity, *VTI* velocity time integral, *AO* aorta, *DA* ductus arteriosus, *BA* brachiocephalic artery, *LCCA* left common carotid artery, *LSA* left subclavian artery.

hypoxia and subsequent complications. Currently, even if significant progress has been made in antenatal sonographic diagnosis of CoA, approximately 20% of fetuses with CoA were typically detected during the second trimester of pregnancy, and over half of CoA cases were confirmed by neonatologists[18,19]. Antenatal diagnosis of CoA can significantly decrease the morbidity and mortality caused by this condition but increase

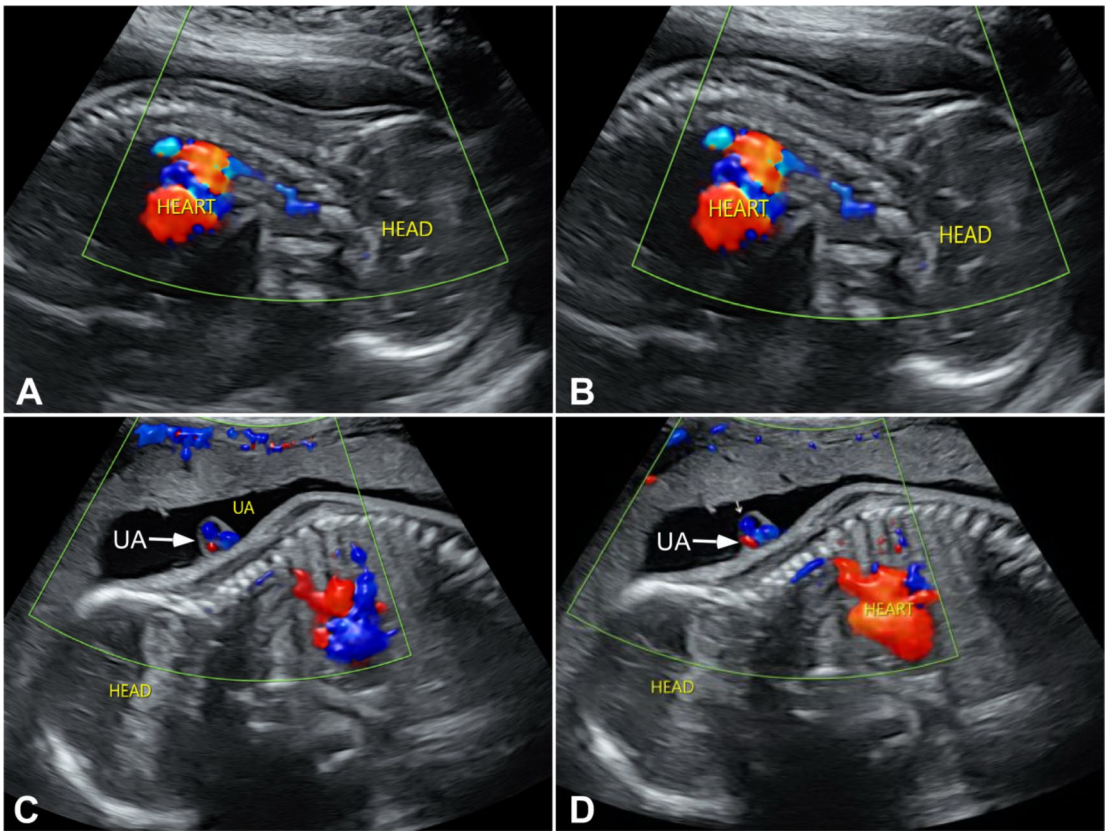

Fig. 6. Fetuses with and without umbilical cord around fetal neck (CAFN). (**A**,**B**) Two fetuses without CAFN were shown. (**C**,**D**) Two fetuses with CAFN (arrow) were shown. The umbilical cord (UA) was shown to surround the fetal neck.

the postnatal outcome. Accurate diagnosis of CoA is necessary, and the rate of correct diagnosis needs to be increased significantly to improve the prognosis.

Evaluation of ventricular dimensions and right and left ventricular disproportion has been used for antenatal prediction of CoA, with dominance of the right-side structures over the left-side ones being associated with the development of CoA[1,20–22], because of blood flow impediment in CoA and subsequently significantly smaller left cardiac structures[20]. Nonetheless, this method has only moderate sensitivity in diagnosing CoA, with a high false-positive rate up to 80% [7]. Especially during late pregnancy, as the foramen ovale is about to close, the right to left shunt decreases and the right heart blood flow increases relatively, resulting in an increase in the right heart size, pulmonary artery/aortic diameter ratio, and DA/aortic isthmic diameter ratio[4,23–25]. The left heart blood flow decreases relatively, and the blood flow through the isthmus also decreases accordingly, causing physiological isthmic stenosis and features of false-positive CoA[23–25]. In addition, in some cases during the middle pregnancy, the foramen ovale is small or the oval valve is long and restricts right-to-left shunting, which may also cause the above effects. Some pathological conditions, such as persistent left superior vena cava merging into the right atrium through the coronary sinus, can limit the ejection of blood from the left atrium to the left ventricle due to the widened coronary sinus[26,27], resulting in reduced left ventricular ejection, decreased blood flow through the isthmus, and a smaller inner diameter of the isthmus[23]. Larger ventricular septal defects can also lead to an increase in the left-to-right shunting and a decrease in the left heart blood flow during fetal development[4]. There are also some situations where the right heart blood flow is obstructed, such as premature constriction of the DA and pulmonary artery stenosis, which may cause imbalance in the ratio of left and right hearts and large arteries. All the above conditions may result in false positive CoA. But with the transition of fetal circulation to infant circulation and the closure of the foramen ovale and DA after birth, the left heart blood flow gradually becomes dominant, and the blood flow through the isthmus also increases accordingly. The thinning of the isthmus caused by fetal physiological conditions will be significantly improved, gradually transitioning to normal (increased volume load), especially after the DA is closed. At this time, the aortic isthmus becomes the only channel for cardiac ejection to the whole body. Newborns with ventricular septal defect will experience an increase in isthmic blood flow and an improvement in the original inner diameter as the defect is closed (naturally or surgically).

In our study, no significant difference was detected in the right and left cardiac structures between the false-positive and false-negative (or positive) fetuses, which has confirmed the uselessness of the cardiac dimensions and ventricular proportion for prenatal diagnosis of CoA. Our study also detected significantly decreased

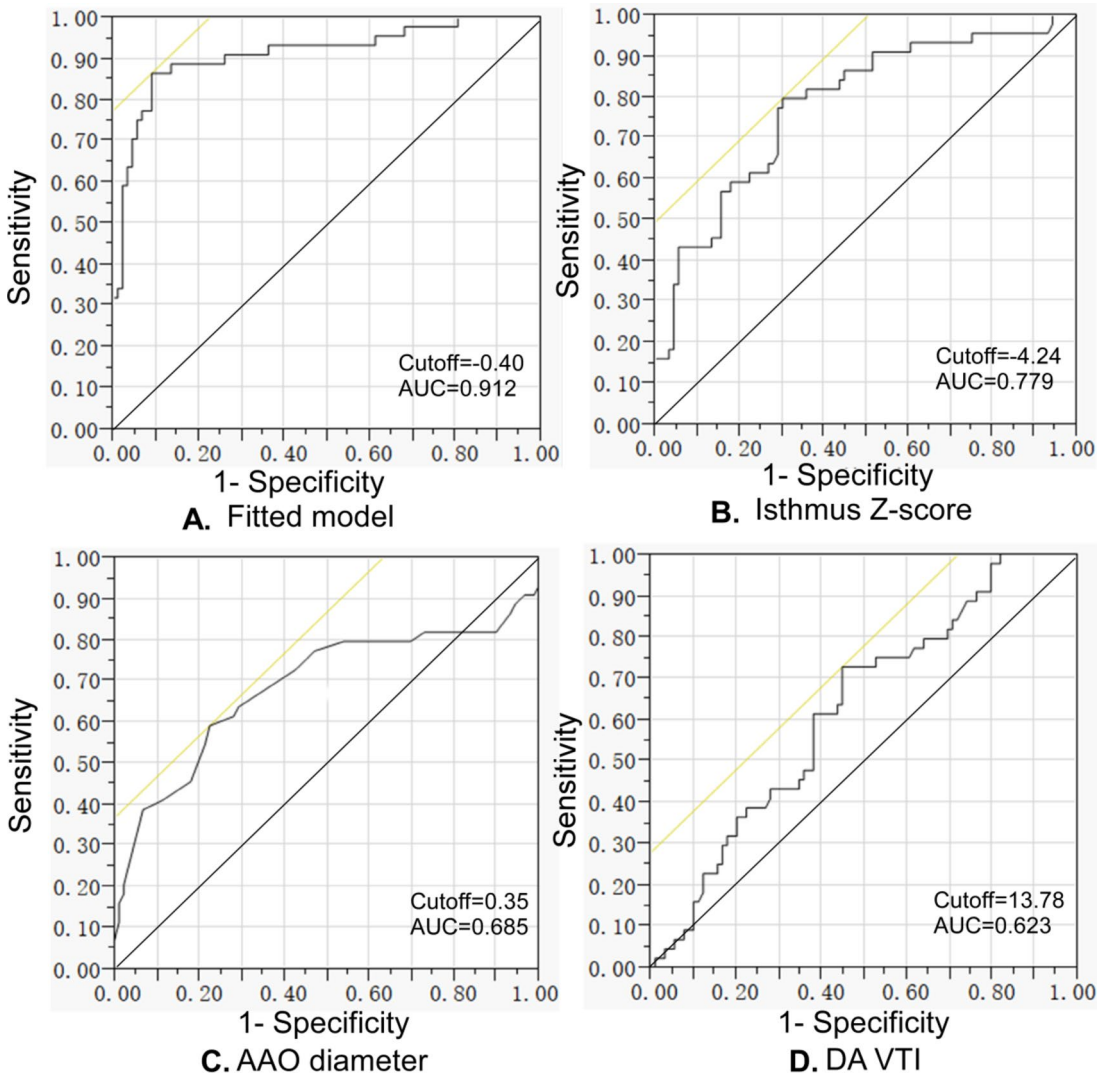

Fig. 7. Receiver operating characteristics (ROC) curve analysis of the fitted model and continuous independent risk factors of coarctation of the aorta (CoA) revealed that the cutoff value, area under the ROC curve (AUC), sensitivity, specificity, positive predictive value, negative predictive value, and Youden index were 0.40, 0.912, 0.864, 0.909, 0.826, 0.930, and 0.773, respectively for the fitted model (**A**), -4.24, 0.779, 0.796, 0.697, 0.565, 0.873, and 0.493, for sagittal view isthmic Z-score (**B**), 0.35, 0.685, 0.591, 0.775, 0.565, 0.793, and 0.276 for ascending aorta (AAO) diameter (**C**), and 13.78, 0.623, 0.727, 0.551, 0.444, 0.803, and 0.278 for ductus arteriosus (DA) velocity time integral (VTI) (**D**).

MV-E, MV-E/A, TV-E and TV-A in CoA positive fetuses as risk factors for CoA presence, but they were not independent risk factors of CoA.

The diameter of MPA and aorta in the third trimester, especially the MPA/aorta diameter ratio, has been used for antenatal diagnosis of CoA, with the ratio of 1.60 or above harboring a sensitivity 83%, specificity 85%, and PPV 62.5% for distinguishing true from false CoA[28]. This approach is an improvement in prenatal diagnosis but is limited only to the third trimester when the conditions for echocardiography scan have been significantly restricted because of the high gestational age[7]. Our study enrolled fetuses with the gestational age of 19–36 weeks, and the diameter ratio of PA/AAO or aorta and the diameter ratio of MPA/AAO (not the PA or MPA diameter) were significantly increased in the CoA positive fetuses. These diameter ratios were also risk factors for CoA presence in the univariate analysis. Nonetheless, they were not independent risk factors of CoA in the multivariate analysis.

The Z-scores of the fetal aortic isthmus have been developed and helpful in diagnosing aortic defects, but cannot be used solely for diagnosis because of clinically significant and unacceptable alterations in the Z-scores with different sonographic instruments and examiners[29]. Significantly lower Z-scores of the AAO and aortic isthmus had been reported to be present in neonates with CoA[2,30]. The mean Z-scores of the isthmus and MV were significantly lower while the MPA and TV Z-scores were significantly higher in CoA fetuses[3]. Our study had confirmed decreases in the Z-scores of the isthmus, aorta and AAO. Although the Z-scores of the isthmus, aorta and AAO were risk factors for CoA, only the isthmic Z-score was an independent risk factor.

The CSAi (carotid to subclavian artery index calculated as the ratio of aortic transverse diameter to the carotid-subclavian artery distance) has been investigated and, a significant decrease in the CSAi was found to be the most sensitive method for CoA detection[7]. The ratio of the LCCA-LSA distance to the distal aortic arch diameter and the Z-score of the peak aortic flow were also explored in a model to predict prenatal CoA presence, which had been reported to perform well in predicting CoA presence after birth[31]. The diameter of the aortic isthmus and transverse arch, the LCCA-LSA distance, and the presence or absence of ventricular septal defect and bicuspid aortic valve had been used to create a model for predicting the need for surgical correction of CoA in newborns, resulting in good PPV and NPV of 86.9% and 90.9%, respectively[32]. In our study, the BA, LCCA and LSA diameter, BA-LCCA and LCCA-LSA distance, aortic diameter at the annulus, transverse aortic arch diameter (3VTV), SV aortic arch diameter at three locations, AAO and DAO diameter, DA and isthmus diameter, LCCA-LSA/aortic diameter, LCCA-LSA/BA-LCCA distance, isthmus displacement between LSA and DAO, isthmus/arch 1–3 diameter, and ratio of isthmus/AAO, DA or DAO diameter were all analyzed. It was found that the aortic and AAO diameter, SV isthmus diameter, 3VTV transverse aortic arch diameter, arch diameter at 3 locations, SV isthmus displacement 1–3, SV isthmus diameter/arch 1 diameter, SV isthmus/AAO or aortic diameter, isthmus/DAO or DA were all significantly dropped while the LCCA-LSA/arch 3 diameter and LCCA-LSA/BA-LCCA distance both significantly rose in CoA positive fetuses compared with false-positive ones, and these parameters were also significant risk factors of CoA presence. However, only AAO diameter was an independent risk factor for CoA presence in the multivariate analysis. The LCCA-LSA distance measured on neonatal echocardiography was reported to be useful in predicting CoA in the presence of a large DA because of a stretch or change in the contour of the transverse aortic arch to the proximal DAO (including the aortic isthmus) in patients with CoA[33,34]. Transverse arch hypoplasia[2] and increased pulmonary valve and PA diameter had been present in neonates with CoA[35]. Decreased 3VTV transverse aortic arch diameter and arch diameter at 3 locations indicated aortic arch hypoplasia in our study. Nonetheless, in prenatal ultrasound evaluation, none of the LCCA/LSA distance, 3VTV transverse arch diameter and SV arch diameters at 3 locations were independent risk factors for CoA as revealed in our study.

Presence of the coarctation shelf was reported to be more common in CoA fetuses than in the controls[3], and the coarctation shelf was found to be a significant independent risk factor for CoA presence in our study. The coarctation shelf indicates an obvious rear infolding in the vessel media and may extend around the total circumference of the aorta. This sign can be detected more frequently after birth when the ductal tissue is believed to surround the aorta constricts during the process of DA closure. Abnormal insertion of the DA into the DAO may play a critical role in CoA development and shaping of the aortic arch, which may cause a significant difference in the angle formed between the aortic segments and the DA in CoA fetuses compared with that in the control[1,36]. It has been reported that the coarctation shelf has a high specificity but a low sensitivity for CoA presence, partially because of the difficulty in visualization on antenatal echocardiography. In our study, the coarctation shelf was found to be an independent risk factor for CoA presence.

The isthmic diastolic and systolic VTIs have been studied[30], and it was reported that the isthmic diastolic and systolic VTI, diastolic/systolic VTI, and diastolic VTI/(diastolic + systolic) VTI were significantly increased in CoA fetuses compared with those in the normal controls and false-positive CoA fetuses. In our study, PA, DA, BA, LCCA, LSA, aorta, DAO, isthmus, diastolic and systolic isthmus, diastolic/systolic isthmus, and diastolic/(diastolic + systolic) isthmus were all investigated, and a significant decrease in the VTI of DAO, systolic isthmus, and DA, but a significant increase in the VTI ratio of diastolic/systolic isthmus, and diastolic/(diastolic + systolic) isthmus were found in CoA fetuses. The DA VTI was an independent risk factor for CoA.

Our study also found significant decreases in the aortic flow volume, ratio of the aortic flow volume to the PA flow volume, DAO and isthmic flow velocity, isthmic flow volume and PSV, ratios of the isthmic flow volume to other flow volume (LCO, CCO, and flow volume of DA, DAO, BA, LCCA, and LSA), and ratio of the isthmic systolic and diastolic flow volume to the estimated weight in CoA positive fetuses. Although abnormal or low flow may cause poor growth of cardiac structures and affect the shape of the aortic arch and subsequent development of CoA[4], none of these flow parameters were independent risk factors of CoA.

In our study, significantly more DA tortuosity was present in false-positive fetuses, whereas significantly more intracardiac malformation, ventricular sepatal defect, extracardiac malformation, and short limbs were found in CoA fetuses. These significant differences may be used to distinguish the false-positive and true positive CoA fetuses. In our study, fetuses with false-positive CoA were included because of the ratio of DA inner diameter to aortic isthmic inner diameter > 1.3 and decreased isthmic diameter (Z-Score < -2) with or without aortic arch dysplasia (transverse arch diameter smaller than 1/2 of the abdominal aortic diameter). The decrease in the isthmic inner diameter and aortic arch dysplasia may limit the blood flow from entering the DAO, leading to blood stasis and subsequent DA tortuosity. Moroever, conditions decreasing the left heart blood flow and restricting the blood flow through the isthmus may cause physiological isthmic stenosis and features of false-positive CoA[23–25]. Some pathological conditions, such as persistent left superior vena cava merging into the right atrium through the coronary sinus[26,27] may result in a smaller inner diameter of the isthmus[23]. Larger ventricular septal defects[4] and premature constriction of the DA and pulmonary artery stenosis may cause imbalance in the ratio of left and right hearts and large arteries and consequenlty false positive CoA. All these conditions may restrict blood flow from entering the distal DAO and cause DA tortuosity.

We investigated the presence of CAFN in our study, with a significantly ($P = 0.04$) increased rate in the CoA false-positive fetuses compared with the true CoA fetuses (34.8% vs. 18.2%). However, we do not think that CAFN mimicks CoA from the ultrasound images (Fig. 5). CAFN did not result in significant ($P > 0.05$) differences in any parameters in the false-positive CoA fetuses, whereas in the true CoA fetuses, CAFN coexisted with significant ($P < 0.05$) decreases in the isthmic flow velocity and PSV. This may indicate that CAFN did not play a very important role in the explanation of our findings in this study even though CAFN has been reported to mimick prenatal CoA in one study[37]. In fetuses with CAFN, the umbilical cord diameter may depend on the

degree to which the umbilical cord wraps around the neck. If the umbilical cord wraps tightly around the fetal neck, the umbilical cord may become narrowed. If the umbilical cord wraps loosely around the fetal neck, it may not be narrowed.

This study had some limitations, including the one-center study design, no randomization, a small cohort of sample, and Chinese subjects enrolled, which may all affect the publication bias and the generalization of the outcomes. Future prospective, randomized, controlled, multi-center studies will have to be conducted involving multiple races and ethnicities for better outcomes.

To sum up, significant differences exist in many ultrasound parameters CoA fetuses, and sagittal view isthmus Z-score, coarctation shelf, ascending aortic diameter, DA VTI independently affect CoA presence. Previous studies have found in CoA the dominance of the right side cardiac structures over the left ones, significant increases in MPA/aorta diameter ratio and isthmus VTI, but significant decreases in the Z scores of AAO, aortic isthmus, MPA and TV, CSAi, transverse arch diameter and PA diameter. Our study has confirmed the above findings but also added new ones: significant increases in MV-E, MV-E/A, TV-E, TV-A, ratios of LCCA-LSA distance /arch 3 diameter and LCCA-LSA/BA-LCCA distance, diameter and VTI ratios of diastolic/systolic isthmus, as well as significant decreases in diameter ratios of PA/AAO or aorta, and MPA/AAO, VTI of DAO, systolic isthmus, and DA, and aortic and isthmic flow volume.

Data availability

The datasets generated and/or analyzed during the current study are not publicly available due to the restriction by the hospital policy but are available from the corresponding author on reasonable request.

Received: 11 June 2024; Accepted: 9 January 2025
Published online: 31 March 2025

References

1. Arya, B. & Maskatia, S. A. Coarctation of the aorta: prenatal assessment, postnatal management and neonatal outcomes. *Semin. Perinatol.* **46**, 151584 (2022).
2. Contro, E. et al. Prediction of neonatal coarctation of the aorta at fetal echocardiography: a scoring system. *J. Matern. Fetal Neonatal Med.* **35**, 4299–4305 (2022).
3. Familiari, A. et al. Risk factors for coarctation of the aorta on prenatal ultrasound: a systematic review and meta-analysis. *Circulation* **135**, 772–785 (2017).
4. Fujisaki, T. et al. Utility of novel echocardiographic measurements to improve prenatal diagnosis of coarctation of the aorta. *Sci. Rep.* **13**, 4912 (2023).
5. Gach, P. et al. Multimodality imaging of aortic coarctation: from the fetus to the adolescent. *Diagn. Interv. Imaging* **97**, 581–590 (2016).
6. Lee, A. et al. Subjective and objective sonographic assessment for the prenatal detection of neonatal coarctation of the aorta. *Fetal Diagn. Ther.* **50**, 98–105 (2023).
7. Zych-Krekora, K., Krekora, M., Grzesiak, M. & Sylwestrzak, O. The predictive value of the csa index in the prenatal diagnosis of aortic coarctation in ultrasound examination performed during the second trimester. *J. Clin. Med.* ;**12** (2023).
8. Garne, E., Stoll, C., Clementi, M. & Euroscan, G. Evaluation of prenatal diagnosis of congenital heart diseases by ultrasound: experience from 20 European registries. *Ultrasound Obstet. Gynecol.* **17**, 386–391 (2001).
9. Galindo, A. et al. Prenatal detection of congenital heart defects: a survey on clinical practice in Spain. *Fetal Diagn. Ther.* **29**, 287–295 (2011).
10. Gomez-Montes, E. et al. Gestational age-specific scoring systems for the prediction of coarctation of the aorta. *Prenat. Diagn.* **34**, 1198–1206 (2014).
11. Matsui, H., Mellander, M., Roughton, M., Jicinska, H. & Gardiner, H. M. Morphological and physiological predictors of fetal aortic coarctation. *Circulation* **118**, 1793–1801 (2008).
12. Power, A., Nettel-Aguirre, A. & Fruitman, D. Fetal right ventricular prominence: Associated postnatal abnormalities and coarctation clinical prediction tool. *Pediatr. Cardiol.* **38**, 1471–1477 (2017).
13. Jowett, V. et al. Sonographic predictors of surgery in fetal coarctation of the aorta. *Ultrasound Obstet. Gynecol.* **40**, 47–54 (2012).
14. Anuwutnavin, S. et al. Prenatal sonographic predictors of neonatal coarctation of the aorta. *J. Ultrasound Med.* **35**, 2353–2364 (2016).
15. International Society of Ultrasound in O et al. Isuog practice guidelines (updated): Sonographic screening examination of the fetal heart. *Ultrasound Obstet. Gynecol.* **41**, 348–359 (2013).
16. Carvalho, J. S. et al. Isuog practice guidelines (updated): fetal cardiac screening. *Ultrasound Obstet. Gynecol.* **61**, 788–803 (2023).
17. Beattie, M., Peyvandi, S., Ganesan, S. & Moon-Grady, A. Toward improving the fetal diagnosis of coarctation of the aorta. *Pediatr. Cardiol.* **38**, 344–352 (2017).
18. Hede, S. V., DeVore, G., Satou, G. & Sklansky, M. Neonatal management of prenatally suspected coarctation of the aorta. *Prenat. Diagn.* **40**, 942–948 (2020).
19. van Velzen, C. L., Ket, J. C. F., van de Ven, P. M., Blom, N. A. & Haak, M. C. Systematic review and meta-analysis of the performance of second-trimester screening for prenatal detection of congenital heart defects. *Int. J. Gynaecol. Obstet.* **140**, 137–145 (2018).
20. Soveral, I. et al. Early cardiac remodeling in aortic coarctation: insights from fetal and neonatal functional and structural assessment. *Ultrasound Obstet. Gynecol.* **56**, 837–849 (2020).
21. Hornberger, L. K., Sahn, D. J., Kleinman, C. S., Copel, J. & Silverman, N. H. Antenatal diagnosis of coarctation of the aorta: a multicenter experience. *J. Am. Coll. Cardiol.* **23**, 417–423 (1994).
22. Quartermain, M. D. et al. Left ventricle to right ventricle size discrepancy in the fetus: the presence of critical congenital heart disease can be reliably predicted. *J. Am. Soc. Echocardiogr.* **22**, 1296–1301 (2009).
23. Tuo, G. et al. Fetal aortic coarctation: a combination of third-trimester echocardiographic parameters to improve the prediction of postnatal outcome. *Front. Pediatr.* **10**, 866994 (2022).
24. Sharland, G. K., Chan, K. Y. & Allan, L. D. Coarctation of the aorta: difficulties in prenatal diagnosis. *Br. Heart J.* **71**, 70–75 (1994).
25. Meng, H. et al. Accurate prenatal diagnosis of coarctation of the aorta by 3-step echocardiographic diagnostic protocol. *BMC Pediatr.* **24**, 552 (2024).
26. Keles, A. et al. Persistent left superior vena cava: why is prenatal diagnosis important? *Fetal Pediatr. Pathol.* **41**, 592–602 (2022).
27. Yonehara, K., Terada, K. & Morine, M. Prenatal diagnosis of persistent left superior vena cava raises suspicion for coarctation of aorta. *Cureus* **14**, e30220 (2022).

28. Slodki, M., Rychik, J., Moszura, T., Janiak, K. & Respondek-Liberska, M. Measurement of the great vessels in the mediastinum could help distinguish true from false-positive coarctation of the aorta in the third trimester. *J. Ultrasound Med.* **28**, 1313–1317 (2009).
29. Pasquini, L. et al. Z-scores of the fetal aortic isthmus and duct: an aid to assessing arch hypoplasia. *Ultrasound Obstet. Gynecol.* **29**, 628–633 (2007).
30. Wang, H. et al. The diastolic and systolic velocity-time integral ratio of the aortic isthmus is a sensitive indicator of aortic coarctation in fetuses. *J. Am. Soc. Echocardiogr.* **32**, 1470–1476 (2019).
31. Wang, H. H. et al. A clinical prediction model to estimate the risk for coarctation of the aorta: from fetal to newborn life. *J. Obstet. Gynaecol. Res.* **48**, 2304–2313 (2022).
32. Bartolacelli, Y. et al. Echocardiographic score to predict neonatal surgery for aortic coarctation in newborns with prenatal suspicion and patent ductus arteriosus. *J. Matern Fetal Neonatal Med.* **36**, 2201654 (2023).
33. Soslow, J. H. et al. A clinical prediction model to estimate the risk for coarctation of the aorta in the presence of a patent ductus arteriosus. *J. Am. Soc. Echocardiogr.* **26**, 1379–1387 (2013).
34. Dodge-Khatami, A., Ott, S., Di Bernardo, S. & Berger, F. Carotid-subclavian artery index: new echocardiographic index to detect coarctation in neonates and infants. *Ann. Thorac. Surg.* **80**, 1652–1657 (2005).
35. Morrow, W. R., Huhta, J. C., Murphy, D. J. Jr. & McNamara, D. G. Quantitative morphology of the aortic arch in neonatal coarctation. *J. Am. Coll. Cardiol.* **8**, 616–620 (1986).
36. Toole, B. J. et al. Importance of relationship between ductus and isthmus in fetal diagnosis of coarctation of aorta. *Echocardiography* **33**, 771–777 (2016).
37. Więckowska, K., Zych-Krekora, K., Słodki, M. & Respondek-Liberska, M. Do umbilical cord wrapped around the fetal body can mimic signs of aortal coarctation? *Prenatal Cardiol.* **1**, 82–86 (2016).

Author contributions

Study design: Guihong Chen, Bu-Lang Gao, Jie Mi; Data collection: Guihong Chen, Na Li, Zhenglun Alan Wei, Wei Zhao, Xijuan Guo, Yu Chen, Xuna Geng, Yuanyuan Peng, Shuping Ge; Data analysis: Guihong Chen, Shuping Ge, Bu-Lang Gao; Supervision: Jie Mi; Writing and review: Bu-Lang Gao; Approval: All authors.

Funding

This study was supported by Shijiazhuang City Science and Technology Research and Development Plan (no. 221200513).

Declarations

Competing interests

The authors declare no competing interests.

Additional information

Supplementary Information The online version contains supplementary material available at https://doi.org/10.1038/s41598-025-86281-8.

Correspondence and requests for materials should be addressed to G.C. or J.M.

Reprints and permissions information is available at www.nature.com/reprints.

Publisher's note Springer Nature remains neutral with regard to jurisdictional claims in published maps and institutional affiliations.